

NFIB promotes cell survival by directly suppressing p21 transcription in *TP53*-mutated triple-negative breast cancer

Rong-Zong Liu, The M Vo, Saket Jain, Won-Shik Choi, Elizabeth Garcia, Elizabeth A Monckton, John R Mackey and Roseline Godbout* 

Department of Oncology, University of Alberta, Cross Cancer Institute, Edmonton, Canada

*Correspondence to: R Godbout, Department of Oncology, Cross Cancer Institute, 11560 University Avenue, Edmonton, Alberta T6G 1Z2, Canada. E-mail: rgodbout@ualberta.ca

Abstract

Triple-negative breast cancer (TNBC) is an aggressive breast cancer subtype with limited treatment options and poor prognosis. There is an urgent need to identify and understand the key factors and signalling pathways driving TNBC tumour progression, relapse, and treatment resistance. In this study, we report that gene copy numbers and expression levels of nuclear factor I B (*NFIB*), a recently identified oncogene in small cell lung cancer, are preferentially increased in TNBC compared to other breast cancer subtypes. Furthermore, increased levels of *NFIB* are significantly associated with high tumour grade, poor prognosis, and reduced chemotherapy response. Concurrent *TP53* mutations and *NFIB* overexpression (z -scores > 0) were observed in 77.9% of TNBCs, in contrast to 28.5% in non-TNBCs. Depletion of *NFIB* in *TP53*-mutated TNBC cell lines promotes cell death, cell cycle arrest, and enhances sensitivity to docetaxel, a first-line chemotherapeutic drug in breast cancer treatment. Importantly, these alterations in growth properties were accompanied by induction of *CDKN1A*, the gene encoding p21, a downstream effector of p53. We show that *NFIB* directly interacts with the *CDKN1A* promoter in TNBC cells. Furthermore, knockdown of combined p21 and *NFIB* reverses the docetaxel-induced cell growth inhibition observed upon *NFIB* knockdown, indicating that *NFIB*'s effect on chemotherapeutic drug response is mediated through p21. Our results indicate that *NFIB* is an important TNBC factor that drives tumour cell growth and drug resistance, leading to poor clinical outcomes. Thus, targeting *NFIB* in *TP53*-mutated TNBC may reverse oncogenic properties associated with mutant p53 by restoring p21 activity.

Copyright © 2018 Pathological Society of Great Britain and Ireland. Published by John Wiley & Sons, Ltd.

Keywords: nuclear factor I; triple-negative breast cancer; apoptosis; drug resistance; p21; *CDKN1A*; transcriptional regulation

Received 29 March 2018; Revised 21 September 2018; Accepted 10 October 2018

No conflicts of interest were declared.

Introduction

Breast cancer is currently divided into four main subtypes: luminal A, luminal B, HER2-enriched, and basal-like (usually negative for ER, PR, and HER2, referred to as triple-negative) [1]. Distinct therapies have been developed for the management of selected breast cancer molecular subtypes, resulting in greatly improved patient survival [2]. However, triple-negative breast cancer (TNBC) remains a challenge because it does not respond to endocrine therapy or other approved targeted agents. *TP53* mutations, found in the majority of TNBCs [3,4], drive tumour progression via a dual mechanism: loss-of-function (tumour suppression activities) and gain-of-function (oncogenic activities) [4,5]. As such, mutant p53 is a target of particular interest for TNBC. However, targeting mutant p53 is challenging because of its vast mutational complexity and our still limited understanding of its functional

networks. The identification of factors that circumvent mutant p53 function is an alternative approach to the direct targeting of mutant p53.

The Nuclear Factor I (NFI) family of transcription factors (NFIA, NFIB, NFIC, NFIX) [6,7] plays important roles in mammary gland development through regulation of key mammary gland-specific genes [8]. NFIs have been implicated in both the promotion and the suppression of human cancers, depending on cancer type and even subtype [9,10]. NFIB in particular is widely expressed in the human body, with knock-out of *Nfib* in mice revealing essential roles in lung and brain development [9,11,12]. Recent studies have shown that NFIB functions as a driver of metastasis and tumour progression in small cell lung cancer (SCLC) [13–15]. In particular, NFIB overexpression in a pRB/p53-inactivated mouse model accelerates small cell lung cancer progression, whereas reduced NFIB expression in this model suppresses cell proliferation and induces apoptosis, suggesting that NFIB cooperates

with pRB/p53 inactivation to promote SCLC progression [16].

Previous reports indicate that *NFIB* gene copy numbers are increased in TNBC [17] and expression levels are upregulated in ER-negative breast tumours and cell lines [18,19]. In this study, we report that *NFIB* is preferentially enriched in TNBC and represents a critical factor regulating cell proliferation/survival by direct suppression of p21 transcription, a key downstream effector of p53. Thus, targeting *NFIB* may mitigate the effects of *TP53* mutations through induction of p21 expression.

Materials and methods

Cell lines and culture conditions

Human breast cancer cell lines were purchased from the American Type Culture Collection (ATCC, Manassas, VA, USA). For chemotherapy drug sensitivity assays, cells were seeded in 24-well plates and cultured for 48 h, followed by 24 h treatment with docetaxel at the specified concentrations in the absence of antibiotics in the culture medium.

Patients and tissue samples

Primary breast cancer samples from 176 treatment-naïve patients were used for gene expression microarray analysis as previously described [20]. Patient material and clinical information were collected under Research Ethics Board Protocol ETH-02-86-17 (Alberta Cancer Research Ethics Committee) in accordance with the Code of Ethics of the World Medical Association. Patients received standardised guideline-based chemotherapy [anthracycline for high-risk node-negative disease and anthracycline plus taxane (docetaxel) for node-positive disease] and hormone therapy.

Gene profiling data and RT-PCR

Total RNA isolation from frozen primary breast tumour biopsies, gene microarray analysis, and data processing were as previously described [20]. The microarray data used in this article can be accessed under GEO accession number GSE22820 (<https://www.ncbi.nlm.nih.gov/geo/query/acc.cgi>). Gene copy numbers or/and mRNA levels in PAM50 molecular subtypes were analysed based on a TCGA [21] or METABRIC [22] gene profiling dataset obtained from cBioportal. The nucleotide sequences of the primers used for RT-PCR are listed in the supplementary material, Table S1. Semi-quantitative RT-PCR conditions were as previously described [23]. Quantitative PCR amplification was performed using EvaGreen 2X qPCR MasterMix-ROX (abm Inc, Richmond, BC, Canada).

siRNA transfection, overexpression, and cell proliferation assays

MDA-MB-435, HCC1806, and BT-20 cells were transfected with 10 nM scrambled (control) or gene-specific (*NFIB* or *CDKN1A*) siRNAs (ThermoFisher, Waltham, MA, USA; sequences are listed in the supplementary material, Table S1) using RNAiMAX transfection reagent (ThermoFisher). For *NFIB* overexpression, BT-474 cells were transfected with either pcDNA3.1 empty vector or pcDNA3.1-HA-*NFIB* using polyethyleneimine. To measure cell proliferation, transfected cells (30 000 cells per well in triplicate for each condition) were counted using a Coulter Particle and Size Analyzer (Beckman Coulter, Mississauga, Ontario, Canada).

Western blot analysis

Forty micrograms of whole cell lysates was separated by SDS-PAGE and transferred to nitrocellulose membranes. Blots were immunostained with anti-*NFIB* (Cat. No. ab11989; 1:1000; Abcam, Cambridge, UK), anti-p21 (Cat. No. 60214-1-Ig; 1:2000; Proteintech, Rosemont, IL, USA), anti-cleaved caspase 3 (Cat. No. 9664; 1:1000; Cell Signaling, Whitby, Ontario, Canada), anti-FABP7 (1:1000) [24] or anti- β -actin (Cat. No. A3854; 1:100 000; Sigma-Aldrich, St Louis, MO, USA) antibodies. Primary antibodies were detected with horseradish peroxidase-conjugated secondary antibodies (Cat. No. 111-035-003; 1:25 000; Jackson ImmunoResearch Laboratories, West Grove, PA, USA) using ECL (β -actin; GE Healthcare, Chicago, IL, USA), ECL prime (cleaved caspase 3; GE Healthcare) or Immobilon (*NFIB*, p21, and FABP7) (MilliporeSigma, Burlington, MA, USA) detection systems.

Immunohistochemical assay

Formalin-fixed, paraffin-embedded TNBC (four tumours) and non-TNBC (four tumours) tissue sections were immunostained with a validated anti-*NFIB* antibody (ThermoFisher; 1:800). The signal was detected using EnVision+ anti-rabbit secondary system (Agilent, Santa Clara, CA, USA).

Gel shift assays

Gel shifts were carried out using an oligonucleotide spanning an NFI binding element located upstream of the human *CDKN1A* gene [25] as previously described [26]. Briefly, 1 μ g of nuclear protein extract was incubated with the [α -³²P]dCTP-labelled probe. For supershift assays, 1 μ l of anti-NFI (Dr Naoko Tanese) [27], 1 μ l of anti-*NFIB* (ThermoFisher), or 1 μ l of anti-TFAP2A (3B5; Developmental Studies Hybridoma Bank, Iowa City, IA, USA) antibodies was added to the binding reaction 10 min after addition of the labelled probe and incubated at room temperature for 30 min.

Chromatin immunoprecipitation

Chromatin immunoprecipitation (ChIP) was carried out as described previously [28]. Immunoprecipitation was carried out in 0.1% SDS sonication buffer with either rabbit IgG or anti-NFIB antibody (Abcam). ChIP DNA was purified and amplified using Phusion[®] Taq polymerase and primers flanking the NFI element of the *CDKN1A* promoter (supplementary material, Table S1). PCR amplification of the human *GAPDH* promoter region served as a negative control.

Statistical analysis

Cell culture experiments involving manipulation of NFIB expression were carried out three or four times, each time in triplicate. Chromatin immunoprecipitations were carried out three times and gel shift experiments two or three times. Selection of the human breast cancer patient cohort was as previously described [29]. All statistical analyses were performed using MedCalc version 12.4.0.0 (MedCalc, MedCalc Software, Ostend, Belgium). One-way ANOVA (when comparing more than two groups) or two-tailed Student's *t*-test (when comparing two groups) was employed for statistical significance testing. For multiple comparisons, controls were normalised to 1 (RT-qPCR levels) or 100% (drug-induced cell growth inhibition). Pearson's correlation analysis was used to determine correlation coefficients between *NFIB* and *CDKN1A* mRNA levels. A chi-square test was used to estimate statistical significance between categorical frequencies. A log-rank test was used to compare Kaplan–Meier overall and recurrence-free survival probabilities between primary breast cancer populations defined by *NFIB* expression levels (stratified as 'low' or 'high' using receiver operating characteristic analysis of our 176-patient gene microarray dataset or the mRNA *z*-scores from the c-Bioportal datasets) or chemotherapy intervention.

Results

Gene copy numbers and NFIB expression are preferentially elevated in TNBC tumours

To examine the expression patterns of *NFI* genes in different molecular subtypes of breast cancer, we first analysed the mRNA levels of each *NFI* gene (*NFIA*, *NFIB*, *NFIC*, *NFIX*) in a TCGA gene profiling dataset [21]. Of all four *NFI* genes analysed, only *NFIB* showed upregulation (*z*-scores > 0) in all breast cancer PAM50 molecular subtypes, with the highest expression levels (*z*-scores = 3.23) in basal-like tumours (Figure 1A–D). In comparison, the *z*-scores for *NFIA*, *NFIC*, and *NFIX* in basal-like tumours were –0.76, –0.77, and 0.68, respectively (Figure 1A–D). As basal-like breast tumours are mainly triple-negative cancers, we then compared the *z*-scores for *NFIB* in TNBC versus non-TNBC tumours and observed a

significant difference between them (3.12 versus 1.52, $p < 0.001$), indicating preferential overexpression of *NFIB* in TNBC (Figure 1E). To verify the findings obtained from the TCGA dataset [21], we also analysed *NFIB* mRNA levels in a gene profiling dataset [Cross Cancer Institute (CCI)] generated from 176 breast cancer patients [29]. *NFIB* mRNA levels were more than three times higher in TNBC than in non-TNBC (2.00 versus 0.60 in geometric means; $p < 0.001$) (Figure 1F and supplementary material, Table S2).

We further examined the relative frequency of *TP53* mutations and *NFIB* overexpression in TNBC using the TCGA dataset. *TP53* was mutated in 76.5 and 26.6% of TNBCs and non-TNBCs, respectively, whereas *NFIB* was overexpressed (*z*-scores > 0) in 88.8 and 44.6% of TNBCs and non-TNBCs, respectively. The frequency of cancers with both *TP53* mutations and *NFIB* overexpression was 77.9% in TNBC, but only 28.5% in non-TNBC ($p < 0.0001$) (Figure 1G), indicating concurrent *TP53* mutation and *NFIB* overexpression in TNBC. We further observed 2.5- to 17.5-fold increases in *NFIB* mRNA levels in tissues of TNBC origin ($n = 5$) compared with non-TNBC ($n = 5$) based on RT-qPCR analysis (Figure 1H).

As *NFIB* gene amplification has been previously reported in small cell lung cancer cells [14], we then examined *NFIB* gene copy numbers in the TCGA breast cancer cohort [21] based on triple-negative status. We found *NFIB* gene copy gains or amplification in 34% of TNBCs, but in only 8% of non-TNBCs (Figure 1I). We also observed a significant correlation between *NFIB* gene copy numbers and mRNA levels in TNBC, but not in non-TNBC (Figure 1J), suggesting that increased gene copy numbers contribute to *NFIB* overexpression in TNBC.

To examine NFIB expression at the protein level, we immunostained eight tumour tissue sections (four TNBC and four non-TNBC) obtained from our 176-patient breast cancer cohort with an NFIB antibody showing no cross-reactivity with other NFI proteins (Figure 2A). NFIB immunoreactivity was observed in all four TNBC tissues, with three of them (MT1337, MT861, MT50) showing strong staining (Figure 2B, upper panel). In contrast, NFIB was not detected in two non-TNBC tissues (MT278, MT330), with weak staining observed in the remaining two non-TNBCs (Figure 2B, lower panel). Both uniform (GT154, MT1337, MT50) and heterogeneous (MT861) distributions of NFIB were observed in positive tissues.

Elevated NFIB RNA levels are associated with high histological tumour grade and poor patient prognosis

Analysis of our 176-patient breast cancer cohort [29] revealed a significant increase in *NFIB* RNA levels in high nuclear ($p = 0.001$), mitotic ($p < 0.0001$), architectural ($p = 0.038$), and overall ($p < 0.0001$) grade tumours compared with low-grade tumours (supplementary material, Figure S1 and Table S2).

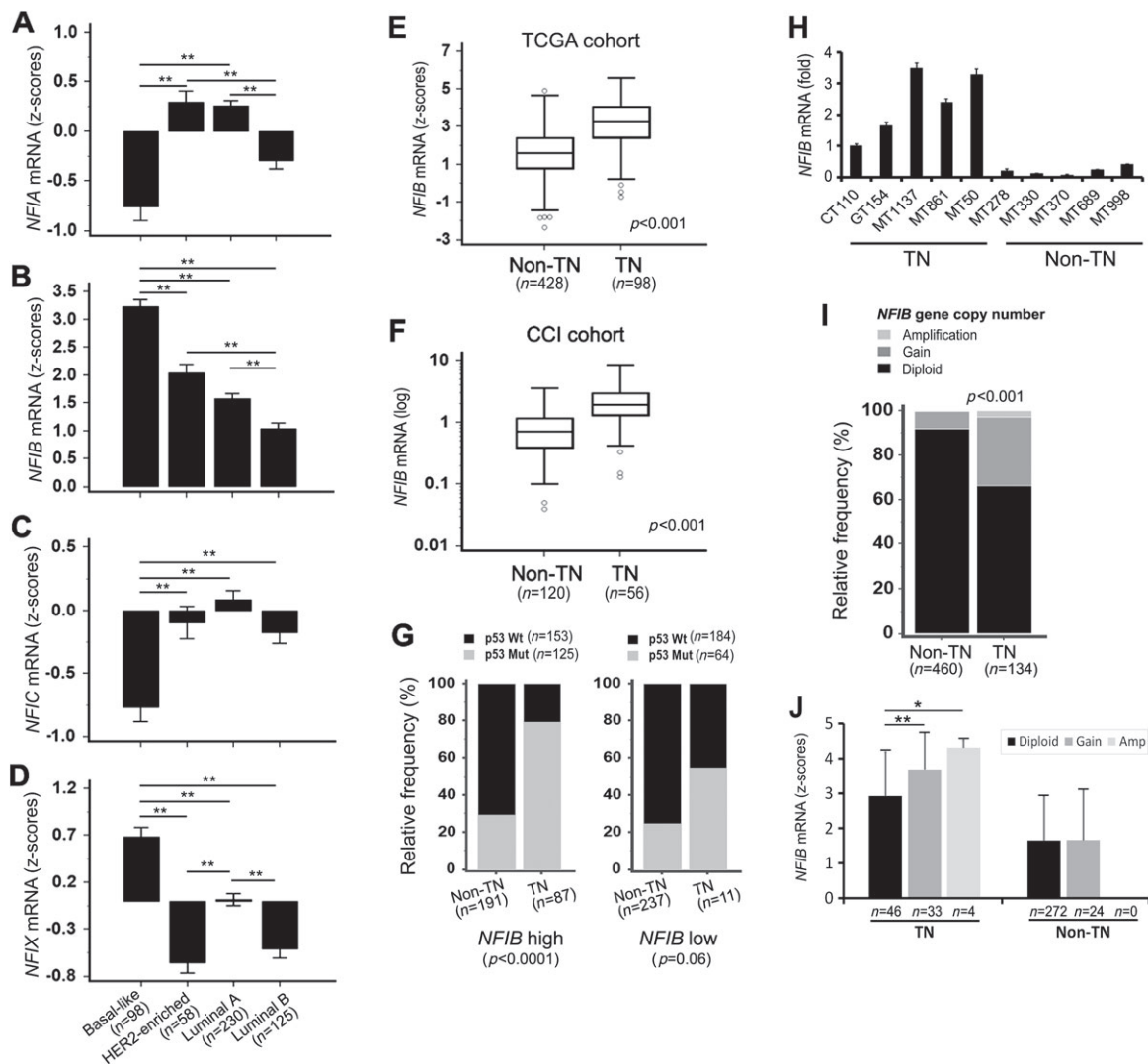


Figure 1. Elevated *NFIB* gene copy numbers and expression levels in basal-like breast cancer or TNBC. (A–D) mRNA levels of *NFIA* (A), *NFIB* (B), *NFIC* (C), and *NFIX* (D) in PAM50 molecular subtypes of human breast cancer. *NFIB* is upregulated in all breast cancer subtypes (z-scores > 0) and is preferentially expressed in basal-like breast cancer (z-scores = 3.2) compared with the other subtypes based on gene profiling data from TCGA [21]. (E, F) *NFIB* mRNA levels are significantly higher in TNBC (TN) than in non-TNBC (non-TN) based on gene profiling data from both the TCGA cohort ($n = 525$) (E) and the Cross Cancer Institute (CCI) cohort ($n = 176$) (F) (GEO accession number: GSE22820). (G) Concurrent *TP53* mutations and *NFIB* overexpression occur in a majority (77.9%) of TNBCs but in only 28.5% of non-TN breast cancers. (H) RT-qPCR shows increased *NFIB* mRNA levels in primary TNBC tissues. (I) Increased *NFIB* gene copy numbers are observed in TNBC. (J) *NFIB* gene copy numbers are positively correlated with *NFIB* mRNA levels in TNBC but not in non-TNBC. n , sample size; HR, hazard ratio; TNBC, triple-negative breast cancer; non-TN, non-triple-negative breast cancer. * $p < 0.05$; ** $p < 0.01$. The z-scores of mRNA levels (in units of standard deviation from the mean of a reference population) shown in A–E, G, J, and the *NFIB* gene copy data shown in I and J, were obtained from TCGA datasets [21]. The mRNA levels shown in F are log-transformed gene microarray signal intensity from our gene microarray dataset (GSE22820, $n = 176$). The cut-off point (1.7239) for the *NFIB* mRNA levels in G was decided by receiver operating characteristic (ROC) analysis.

Significantly increased *NFIB* RNA levels were also observed in tumours with high Ki-67 immunoreactivity (positivity $\geq 15\%$), indicative of cell proliferation [30] (supplementary material, Figure S1), suggesting a possible link between *NFIB* and tumour cell growth. Kaplan–Meier patient survival curves generated for *NFIB*-high and *NFIB*-low patients indicated that elevated *NFIB* levels were significantly associated with both lower overall (HR = 2.46, $p = 0.0023$) and recurrence-free (HR = 1.72, $p = 0.0157$) survival probabilities (Figure 2C). Next, we performed survival analysis on basal-type ($n = 199$, mainly TNBC)

and luminal (non-TNBC) patients ($n = 1445$) using the METABRIC dataset [22]. We observed a strongly unfavourable (HR = 5.59, $p = 0.006$) and a slightly favourable (HR = 0.80, $p = 0.001$) prognostic association with *NFIB* levels in basal and luminal populations, respectively (Figure 2D), indicating that *NFIB* may represent a TNBC-specific adverse factor.

Depletion of *NFIB* in TNBC cells inhibits cell proliferation and induces p21 and cleaved caspase 3. *NFIB* promotes cell proliferation and senescence and inhibits apoptosis in small cell lung cancer cells

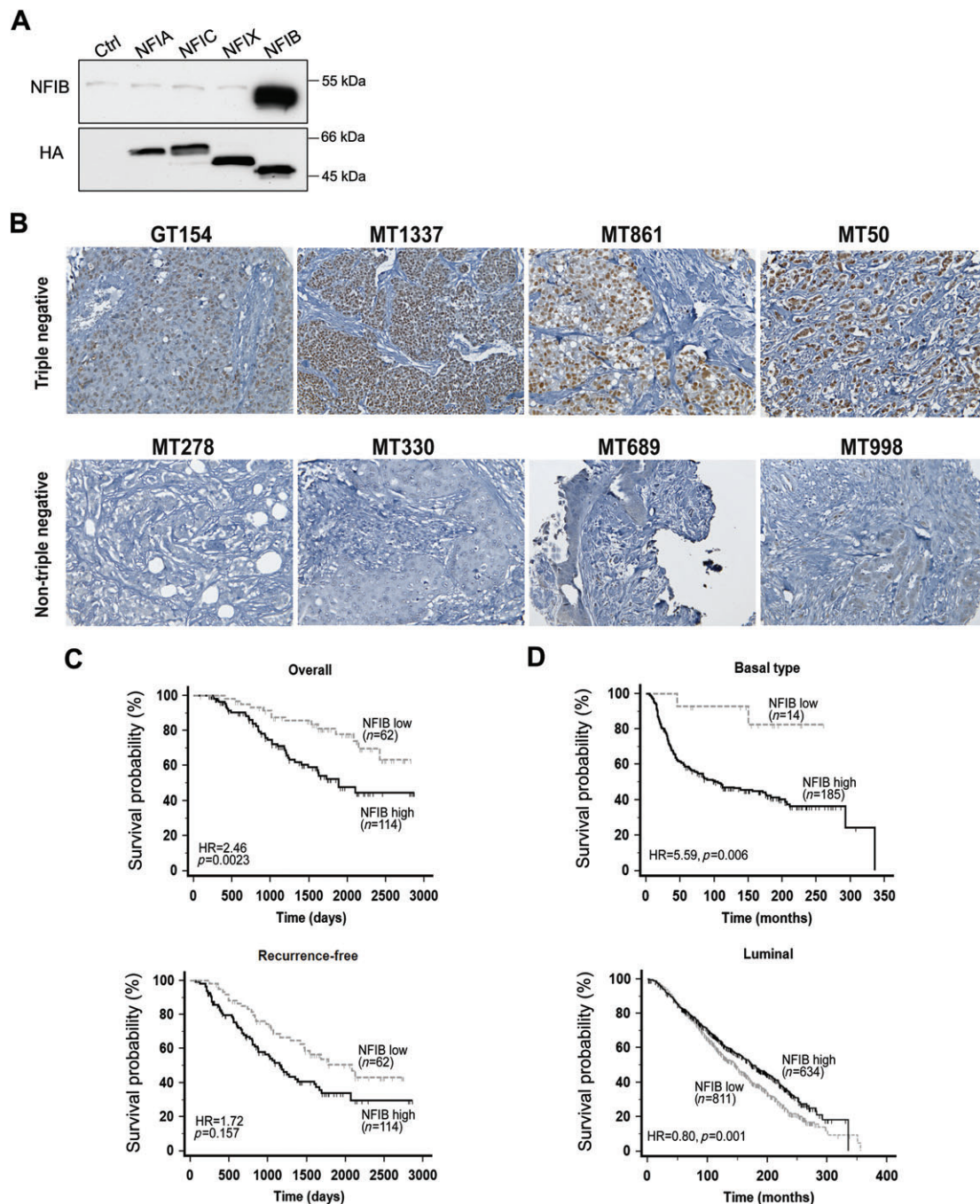


Figure 2. NFIB in breast tumour tissues and prognostic significance of *NFIB* expression in breast cancer patient cohorts. (A) Western blots showing immunoreactivity of the NFIB antibody to HA-tagged NFIB-transfected U251 cells, but not to HA-tagged NFIA-, NFIC-, and NFIX-transfected U251 cells. Cells were harvested 48 h after transfection. (B) Immunohistochemical analysis of four TNBCs (GT154, MT1337, MT861, MT50) (upper panel) and four non-TNBCs (MT278, MT330, MT689, MT998) (lower panel). Tissues were counterstained with haematoxylin (blue). A strong positive signal (brown staining) is observed in TNBC but not in non-TNBC tissues. All eight tumour tissues were from the 176-patient breast cancer cohort. (C) Kaplan–Meier log-rank test shows that high *NFIB* mRNA levels were significantly associated with reduced overall and recurrence-free patient survival ($n = 176$; GEO microarray data accession number: GSE22820). (D) Survival curves generated in subpopulations with basal-type or luminal tumours from the METABRIC breast cancer cohort [22]. The cut-off points for *NFIB* mRNA levels (in z-scores) were determined by ROC analysis using survival status as a classification factor (C, 1.7239) or z-scores (D, 0).

[14]. In primary breast cancers, we observed a significant positive correlation between *NFIB* expression, mitotic tumour grade, and Ki-67 immunoreactivity (supplementary material, Figure S1). To address the possibility that NFIB confers survival and proliferation potential to TNBC cells, we depleted NFIB in three

TP53-mutated TNBC cell lines that naturally express NFIB (MDA-MB-435, HCC1806, and BT-20) (supplementary material, Figure S2) using two different siRNAs. RT-qPCR analysis showed 78–96% reductions in *NFIB* transcript levels after siRNA transfection in different cell lines (Figure 3A–C). Depletion of NFIB

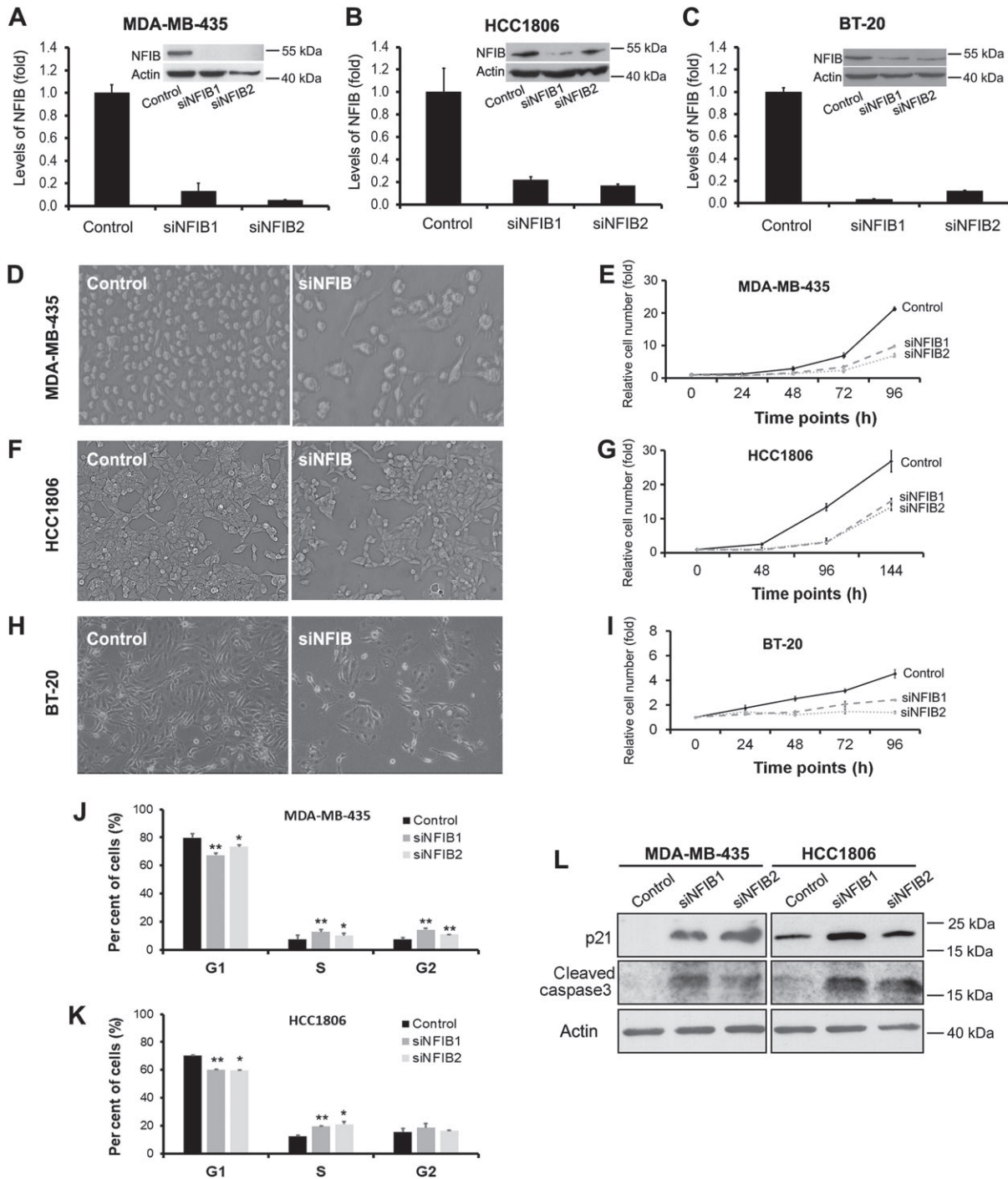


Figure 3. NFIB depletion in *TP53*-mutated TNBC cell lines suppresses cell proliferation and induces p21 activity. (A–C) Depletion of *NFIB* mRNA in MDA-MB-435 (A), HCC1806 (B), and BT-20 (C) was verified by RT-qPCR. Reduced NFIB protein levels in siNFIB-transfected TNBC cells was verified by western blotting (A–C, insets). (D–I) Cell proliferation was significantly inhibited by NFIB depletion in TNBC cell lines MDA-MB-435 (D, E), HCC1806 (F, G), and BT-20 (H, I). (J, K) Flow cytometry analysis showed significant decreases in the percentage of cells in G1 phase, with accompanying increases in the percentage of cells in the S/G2 phases, upon NFIB knockdown in MDA-MB-435 and HCC1806 cells. Cells were harvested when they reached ~80% confluence. (L) Western blot analysis showing concurrent induction of p21 and cleaved caspase 3 in MDA-MB-435 and HCC1806 after NFIB depletion. Cells for RT-PCR and western blotting were harvested 48 h after siRNA transfection. * $p < 0.05$; ** $p < 0.01$.

protein was verified by western blotting (Figure 3A–C, insets). Cell proliferation assays showed a more than 50% reduction in cell numbers after NFIB depletion for all three cell lines 4 days after plating (Figure 3E,G,I). In addition, we observed changes in cell morphology upon NFIB knockdown, particularly in MDA-MB-435

and BT-20 cells (Figure 3D,F,H). NFIB-depleted cells were larger and had a flattened shape compared with control cells. Flow cytometry analysis of MDA-MB-435 and HCC1806 showed increased proportions of cells in the S/G2 phases of the cell cycle upon NFIB depletion suggesting a role for NFIB in cell cycle progression

through S/G2 (Figure 3J,K). No significant changes in cell cycle distribution were observed upon NFIB depletion in BT-20 cells (data not shown).

p21 is an important regulator of cell proliferation and survival in TNBC cells under various stimulatory pathways [31–33]. We therefore examined p21 protein levels upon NFIB depletion. p21 was significantly induced in MDA-MB-435 cells and HCC1806 cells upon NFIB depletion (Figure 3L). In contrast, p53 levels were not affected by NFIB knockdown (data not shown), suggesting that the observed increase in p21 is independent of p53 which is mutated in MDA-MB-435 and HCC1806 [34]. We also observed induction of the cell apoptosis marker cleaved caspase 3 [35] upon NFIB depletion in both MDA-MB-435 and HCC1806 (Figure 3L), indicating that apoptosis contributes to the cell growth inhibition observed in NFIB knockdown cells. As we show later (Figure 6), p21 levels are naturally higher in p53-mutated BT-20 than in either MDA-MB-435 or HCC1806, with NFIB knockdown resulting in only a slight increase in p21 levels.

NFIB attenuates chemotherapy sensitivity

TNBC patients show variability in their response to chemotherapy, underlying the need to understand the molecular mechanisms driving chemotherapeutic response. NFIB overexpression has previously been associated with increased resistance to chemotherapy drugs in cancer cell lines [36]. We therefore tested the effect of docetaxel (DOC), one of the most active chemotherapy agents used in the treatment of invasive breast cancer, on cell proliferation in NFIB-depleted TNBC cell lines. Control and NFIB-depleted MDA-MB-435 and HCC1806 cells all showed DOC-induced inhibition of cell proliferation in a dose-dependent manner; however, NFIB-depleted cells were significantly more sensitive to DOC treatment (Figure 4A,B). BT-20 cells transfected with scrambled siRNA (control) exhibited no growth inhibition in the presence of DOC, whereas NFIB-depleted cells showed 22% and ~40% growth inhibition when treated with 25 nM ($p < 0.05$) and 50 nM ($p < 0.01$) DOC, respectively (Figure 4C). Interestingly, overexpression of NFIB in BT-474, a *TP53*-mutated luminal cell line, did not alter cell response to docetaxel (supplementary material, Figure S3). FABP7 and p21 levels were not affected by NFIB overexpression in BT-474. The lack of an effect in this cell line could be due to the fact that the cells already express endogenous NFIB or may reflect a molecular subtype-dependent role for NFIB in breast cancer.

We used our 176-patient cohort to further examine whether the correlation between NFIB status and chemosensitivity might also apply to breast cancer patients. Patients who received chemotherapy ($n = 50$: 13 ER-negative; 37 ER-positive) had improved prognosis (HR = 2.19, $p = 0.003$) compared with those who did not receive chemotherapy ($n = 126$: 51 ER-negative; 75 ER-positive) (Figure 4D). Notably, this effect

was magnified in the subpopulation of patients with low levels of *NFIB* ($n = 62$) (HR = 8.81, $p < 0.0001$) (Figure 4E), with the effect of chemotherapy becoming insignificant (HR = 1.6, $p = 0.12$) in the population with high levels of *NFIB* ($n = 114$) (Figure 4F).

Next, we examined the effect of NFIB depletion and DOC treatment on p53, p21, caspase 3, and FABP7 protein levels in MDA-MB-435 and HCC1806 cells. As also observed in Figure 3L, p21 and cleaved caspase 3 were markedly induced upon NFIB depletion, whereas the levels of FABP7, a known NFI target [27,37] and a TNBC marker [26], were reduced upon NFIB depletion (Figure 4G,H). DOC treatment increased the levels of p21 (control) and caspase 3 (control and NFIB-depleted), but had no effect on FABP7. There was no significant change in mutant p53 levels upon either NFIB knockdown or DOC treatment. These findings suggest that elevated NFIB levels in TNBC may cause chemotherapy resistance by modulating cell survival pathways.

NFIB regulates *CDKN1A* transcription in TNBC cells

As p21, encoded by the *CDKN1A* gene, was induced in NFIB-depleted TNBC cells independently of p53, we speculated that *CDKN1A* transcription may be directly suppressed by NFIB in TNBC cells. We therefore used gel shift and supershift assays to examine the binding of NFIB to a putative NFI regulatory element [25] in the *CDKN1A* promoter (Figure 5A). Nuclear protein–DNA probe complexes (labelled NFI + P) were observed in all three cell lines examined (MDA-MB-435, HCC1806, and BT-20) (lanes 2 in Figure 5B–D). Addition of 50× and 100× cold probe (lanes 3 and 4 in Figure 5B–D) or NFI consensus binding sequence DNA (lanes 4 and 5 in Figure 5F) effectively competed with the labelled probe, with little to no signal detected, indicating probe-specific interaction. Addition of either a pan-specific NFI antibody or NFIB antibody, but not TFAP2A antibody, to the reaction resulted in a supershifted band (SC), demonstrating the presence of NFIB in the binding complex (Figure 5B–D,F).

Next, we carried out a gel shift assay using nuclear lysates prepared from control and NFIB-depleted MDA-MB-435, HCC1806, and BT-20 cells. The NFI-probe binding complex was absent (MDA-MB-435) or markedly reduced (HCC1806 and BT-20) in NFIB-depleted cells (Figure 5E), suggesting a specific interaction between NFIB and the region of the *CDKN1A* promoter harbouring the NFI binding site. RT-qPCR further showed a 2–5× (MDA-MB-435), 4.5× (HCC1806) or 1.5–2× (BT-20) increase in *CDKN1A* mRNA levels in NFIB-depleted cells compared with control cells (Figure 5G), providing additional evidence for suppression of *CDKN1A* transcription by NFIB. Finally, based on gene expression microarray analysis of our 176-patient breast cancer cohort, we observed a significant negative correlation ($p = 0.02$) between *NFIB* and *CDKN1A* RNA levels in TNBC, but not in non-TNBC ($p = 0.30$) (Figure 5H).

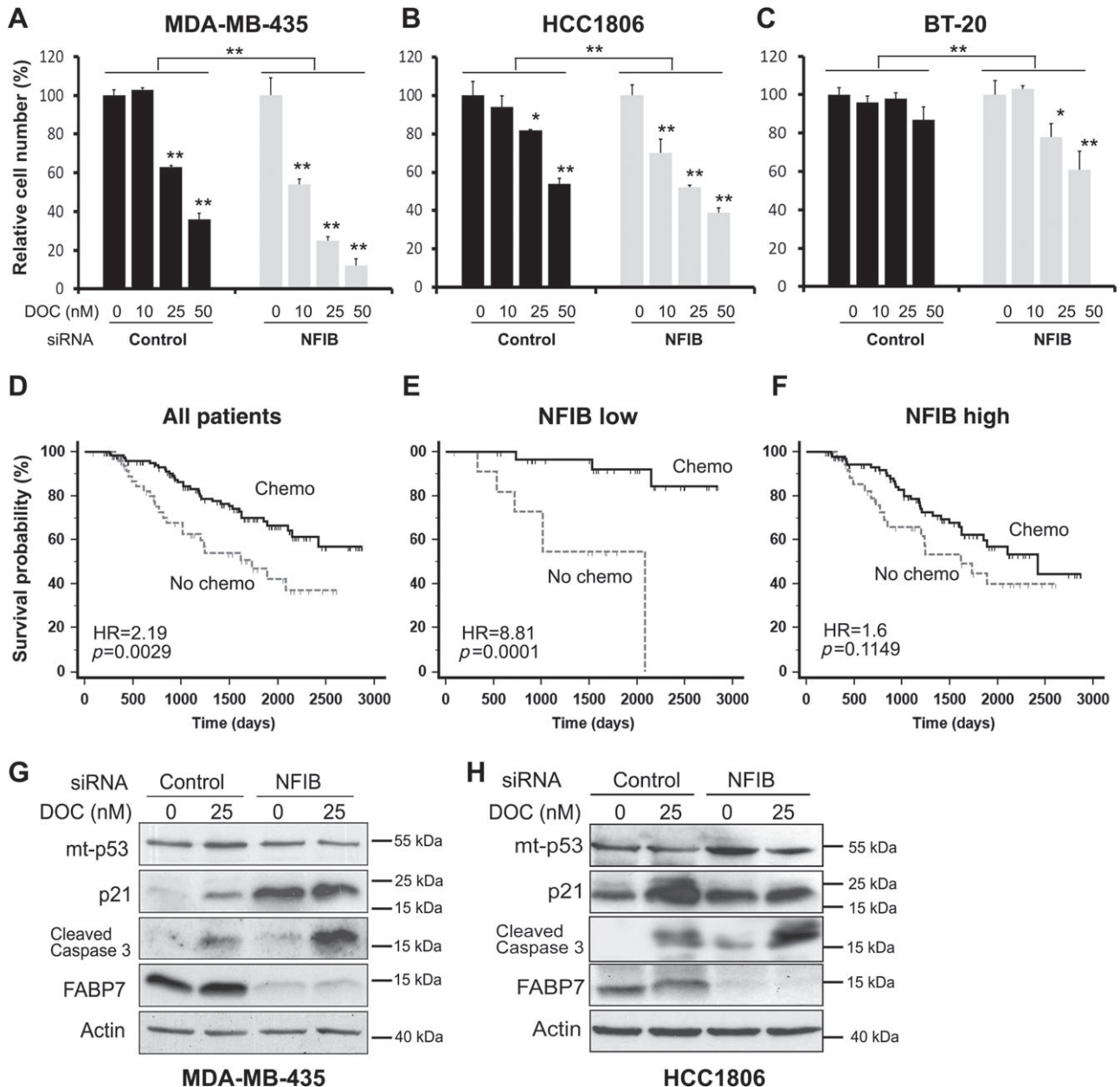


Figure 4. NFIB promotes TNBC cell resistance to the chemotherapy drug docetaxel. (A–C) NFIB-depleted cells show significantly enhanced docetaxel (DOC)-induced cell proliferation inhibition compared with cells transfected with scrambled siRNA (control) in MDA-MB-435 (A), HCC1806 (B), and BT-20 (C) cells. (D–F) Patients treated with chemotherapeutic drugs (chemo) had a significantly better prognosis (with hazard ratio HR = 2.19) compared with patients who received no chemotherapy (no chemo) when the whole patient cohort with primary breast cancer was analysed (D). A considerably higher hazard ratio (HR = 8.81) was observed in the subpopulation with low NFIB levels (E). This effect was lost ($p=0.1149$) in the subpopulation with high NFIB levels (F). The cut-off point (0.1739) for *NFIB* mRNA levels (in normalised microarray signal intensity) was determined by ROC analysis using survival status as a classification factor. (G, H) Western blot analysis showing changes in p21, cleaved caspase 3, and FABP7 levels after NFIB depletion and DOC treatment in MDA-MB-435 and HCC1806 cells. * $p < 0.05$; ** $p < 0.01$.

To demonstrate *in vivo* occupancy of NFIB at the *CDKN1A* promoter, we carried out chromatin immunoprecipitation (ChIP) with anti-NFIB antibody using MDA-MB-435 breast cancer cells. PCR primers flanking the putative NFI binding element in the *CDKN1A* promoter (Figure 5I, upper panel) generated a product of the correct size in the anti-NFIB antibody lane, with a barely detectable band in the control IgG lane (Figure 5I, lower panel). The observed preferential binding of NFIB to the *CDKN1A* promoter sequences containing the

NFI element suggests a direct regulatory relationship between NFIB and p21 in TNBC.

p21 is required for cell growth inhibition and enhanced chemotoxicity in NFIB-depleted TNBC cells

To further investigate whether p21 is a direct downstream effector of NFIB, we transfected MDA-MB-435, HCC1806, and BT-20 cells with siRNAs targeting

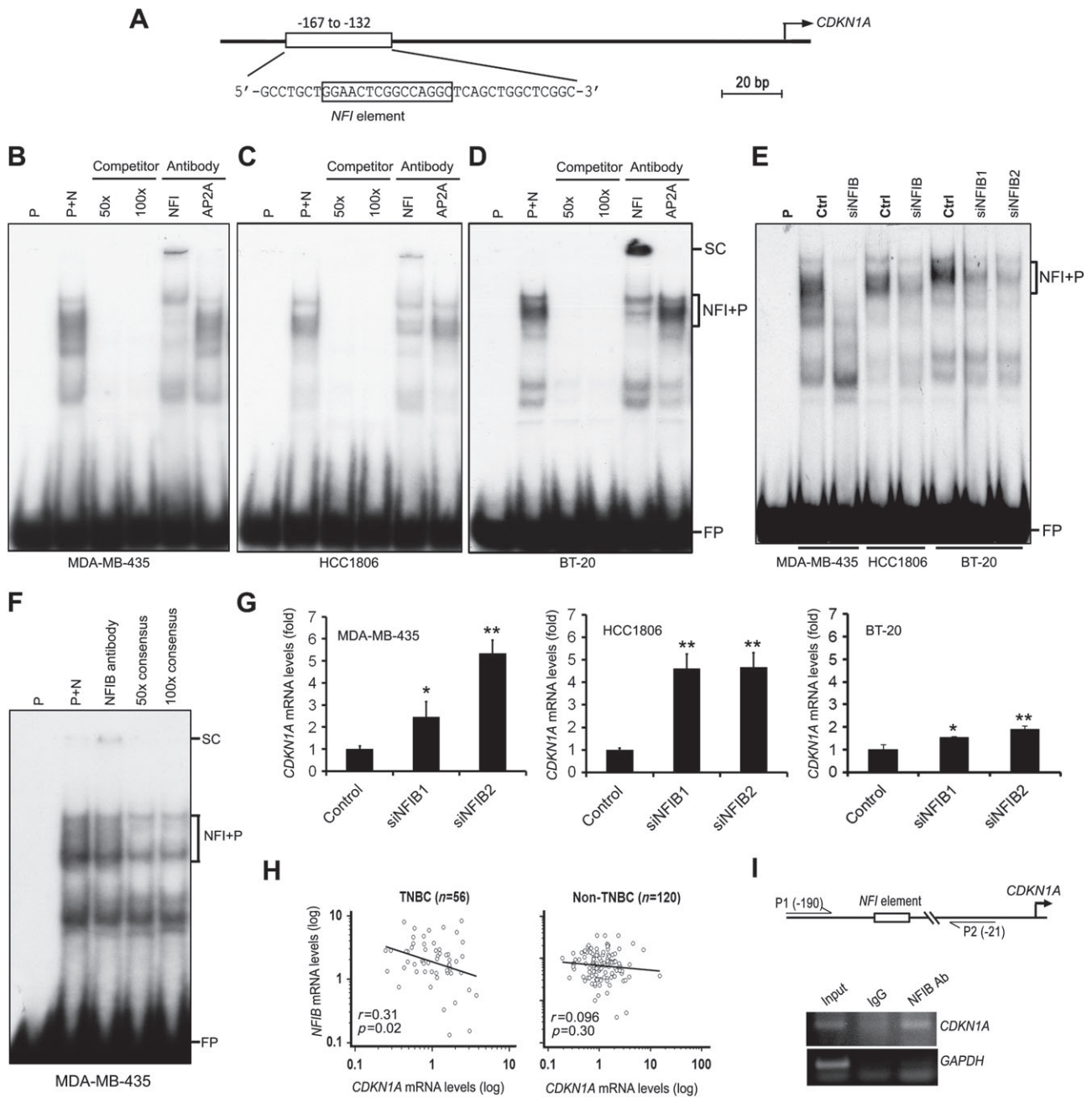


Figure 5. Regulation of *CDKN1A* transcription by NFIB. (A) The sequence of the oligonucleotide used as the probe for the gel shift assays is indicated. The NFI binding element [25] relative to the transcription start site (arrow) of *CDKN1A* transcript variant 1 (NM_00389) is shown in the boxed region. (B–D) Nuclear protein extracts (N) prepared from MDA-MB-435 (B), HCC1806 (C), and BT-20 (D) form a complex (NFI + P) with the ³²P-labelled oligonucleotide probe (P). Unlabelled oligonucleotide competitor in 50x and 100x excess eliminates the protein–DNA complex observed in the N + P lanes. A supershifted complex (SC) is detected with a pan-NFI antibody, but not with an antibody against transcription factor TFAP2A. (E) NFIB depletion results in a significant decrease in the shifted NFI complex (NFI + P) in all three cell lines tested. (F) A supershifted complex (SC) is detected with a validated NFIB antibody. A 50x and 100x excess of an unlabelled consensus NFI–DNA binding element (5′-ATTTTGGCTTGAAGCCAATATG-3′) effectively competed out the protein–DNA complex observed in the N + P lane. (G) Upregulation of *CDKN1A* transcription upon NFIB depletion in MDA-MB-435, HCC1806, and BT-20 cells was measured by RT-qPCR. Cells were harvested 48 h after siRNA transfection. (H) There is a negative correlation between *CDKN1A* and *NFIB* mRNA levels in primary TNBC but not in non-TNBC based on gene microarray analysis. (I) NFIB occupancy of endogenous *CDKN1A* promoter detected by chromatin immunoprecipitation (ChIP). Upper panel: schematic representation of the region upstream of the *CDKN1A* gene containing an NFI binding site. The location of the primers (P1 and P2) used to amplify the region surrounding the NFI binding site is shown. Lower panel: DNA immunoprecipitated with rabbit anti-NFIB antibody or rabbit IgG was PCR-amplified using P1 and P2 primers. PCR products were electrophoresed in a 2% agarose gel. A band of the correct size enriched in the NFIB antibody lane is shown. Input DNA for the immunoprecipitation was used as a positive control for the PCR amplification. PCR amplification of the human *GAPDH* promoter was performed as a negative control for the NFIB immunoprecipitation. kb, kilobase pairs; *n*, sample size; *r*, correlation coefficient; **p* < 0.05; ***p* < 0.01.

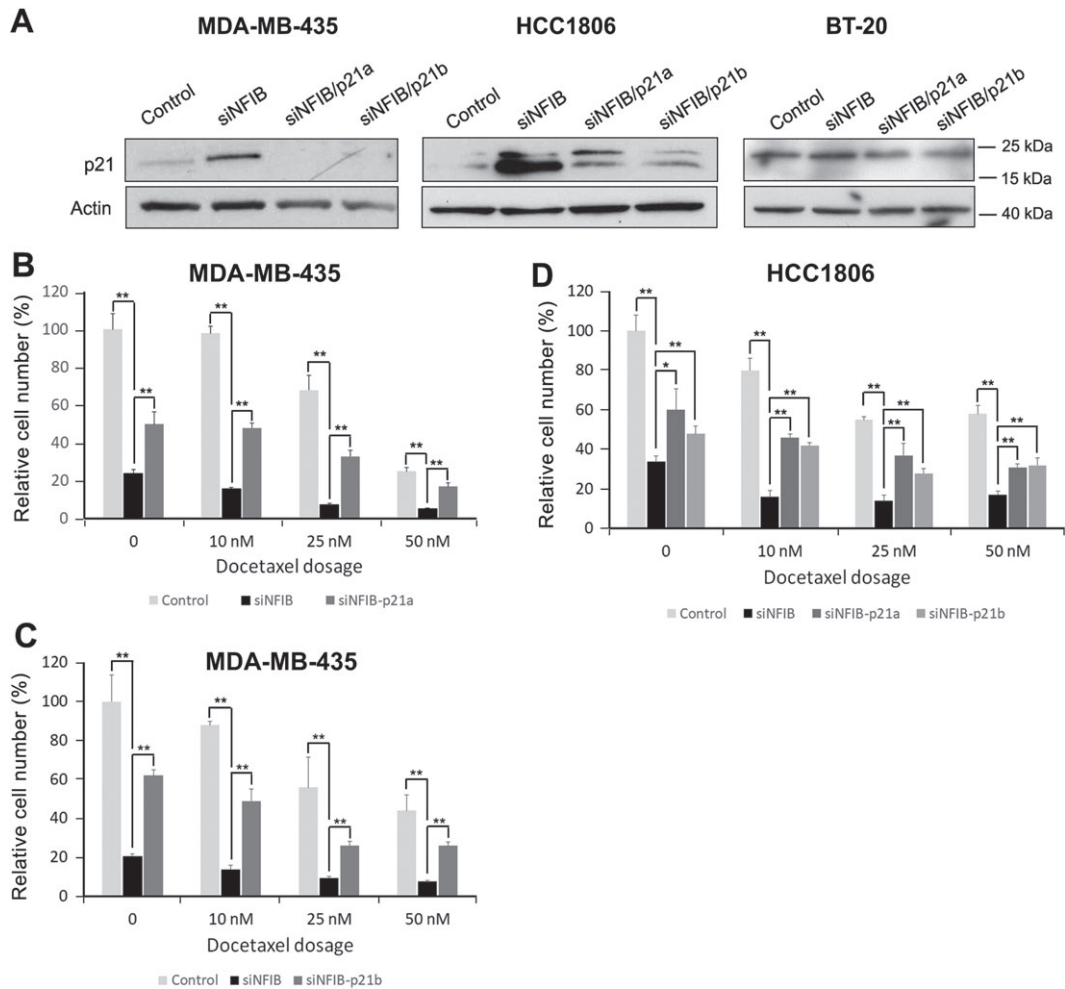


Figure 6. Effect of p21 depletion on cell growth and chemosensitivity in NFIB-depleted cells. MDA-MB-435, HCC1806, and BT-20 cells were transfected with scrambled siRNA (control), siRNA targeting NFIB (siNFIB) or siRNAs targeting both NFIB and p21 (siNFIB/p21a and siNFIB/p21b). (A) Western blot showing induction of p21 upon NFIB depletion in MDA-MB-435, HCC1806, and BT-20, and absence of p21 induction upon NFIB/p21 co-depletion. For these experiments, cells were harvested 2 days after transfection. Similar results were obtained when we used scrambled siRNA to compensate for the total amount of siRNA added to each plate. (B) Proliferation of control, NFIB-depleted, and NFIB/p21a-co-depleted MDA-MB-435 cells treated with docetaxel at the indicated concentrations. Cells were plated in 24-well plates in triplicate after siRNA transfection, cultured for 2 days in normal medium, and counted 24 h after docetaxel treatment. Cell numbers (normalised to scrambled siRNA-transfected control cells in the absence of docetaxel) were significantly reduced in NFIB-depleted cells. This inhibitory effect was significantly (albeit partially) reversed in NFIB/p21a-co-depleted cells at all docetaxel dosages examined. (C) Similar results in MDA-MB-435 were observed with a second p21 siRNA (p21b). (D) Proliferation of control, NFIB-depleted, NFIB/p21a-co-depleted, and NFIB/p21b-co-depleted HCC1806 cells treated with docetaxel at the indicated concentrations. The results are similar to those observed for MDA-MB-435 cells. Statistical significance was examined using Student's *t*-test. **p* < 0.05; ***p* < 0.01.

either NFIB or both NFIB and p21. As expected, p21 was markedly upregulated upon NFIB depletion in both MDA-MB-435 and HCC1806 cells, but was not increased in BT-20 (Figure 6A). Reversal of p21 upregulation was observed in NFIB/p21-co-depleted cells in all three cell lines (Figure 6A). Importantly, the cell growth inhibition observed with NFIB depletion was significantly (albeit partially) reversed upon co-depletion of NFIB and p21, with or without docetaxel treatment in MDA-MB-435 and HCC1806 cells (Figure 6B,D). Inhibition of cell growth upon NFIB depletion with reversal upon co-depletion of NFIB and p21 was also observed using a second siRNA targeting a different region of the p21 transcript (p21b) (Figure 6C,D). However, there was no reversal of DOC-induced cell growth inhibition in

NFIB/p21-co-depleted BT-20, likely due to the small induction in p21 expression observed upon NFIB knock-down in these cells (Figure 6A and data not shown). These results point to a direct causative link between NFIB depletion, p21 induction, and DOC-induced growth inhibition.

Discussion

Our study indicates that NFIB is a driver of cell proliferation/survival and treatment resistance in TNBC cells through direct suppression of a key target gene, *CDKNA1*. The tumour-promoting effect of NFIB is further evidenced by the significant association of its elevated expression levels with high histological grade,

Ki-67 immunoreactivity, chemoresistance, and poor patient prognosis in breast cancer patient cohorts. We propose that loss of p21 due to prevalent *TP53* mutations and NFIB overexpression in TNBC is an important mechanism underlying TNBC cell growth, chemoresistance, and poor clinical outcomes (supplementary material, Figure S4).

NFIs play different roles depending on cellular or tissue context. For example, NFIs that promote differentiation during development can also promote survival of stem cells in adults [38]. In cancer, NFIs can have oncogenic roles (as demonstrated here) or tumour suppressor roles (for recent reviews, see refs 9 and 10). Paradoxical roles of NFIs may be attributed to cellular/molecular context, structural variations, mutations, and post-translational modifications [10].

The function of NFIs in breast cancer remains poorly understood. Studies on the role of NFIB in breast cancer have primarily focused on gene fusion events [9,10]. For example, *NFIB-MYB* gene fusion typically occurs in breast adenoid cystic carcinoma (AdCC), a rare type of TNBC. *NFIB-MYB* fusion leads to elevated levels of functional MYB and disruption of NFIB function. Interestingly, in contrast to the majority of TNBCs which express wild-type NFIB and have a poor prognosis, AdCCs are typically low-grade cancers with indolent clinical behaviour and excellent prognosis [39], in keeping with NFIB being an adverse factor in TNBC. The only other functional investigation of NFIB in breast cancer was carried out in the HER2-overexpressing cell line HCC1954. In agreement with our findings, NFIB knockdown in this cell line resulted in decreased proliferation and increased apoptosis with a greater percentage of cells in S/G2 phases of the cell cycle compared with control cells [18].

A well-known mechanism of p53 action is through regulation of its downstream target *CDKN1A*, which encodes p21. While inhibition of p21 expression is usually associated with loss of p53 activity, upregulation of transcriptional suppressors of p21 can also play an important role in the disruption of p21 function [40]. p21 serves as a downstream effector of other tumour suppressors, such as BRCA1, TGF- β , and Wnt-1 [40], suggesting that it has anti-tumour activities independent of p53. In keeping with the idea that restoring p21 function in *TP53*-mutated tumours could be of significant benefit to a subset of cancer patients, clinical cohort analyses combining p21 expression and p53 status indicate that p21-positive and p53-negative patients have a more favourable prognosis than p21 and p53-double-positive or p21-negative and p53-positive patients in small cell lung cancer (SCLC) [41] and ovarian cancer [42]. As such, identification and targeting critical *CDKN1A* transcriptional suppressors may restore p21 function and overcome the deleterious effects of *TP53* mutations, which occur in 60–88% of TNBCs or basal-like breast cancers [4]. Our findings suggest that NFIB represents such a negative regulator of p21 and is therefore a potential therapeutic target for TNBC.

Taxanes and anthracyclines are important chemotherapeutic agents for TNBC patients, with different efficacies observed in subgroups of TNBC [43]. In particular, breast cancer patients are prone to developing resistance to docetaxel, a potent taxane widely used in the clinic [44]. We have shown that NFIB contributes to resistance to docetaxel in TNBC cells, with significant enhancement of cell response to docetaxel observed upon NFIB depletion in all three TNBC cell lines tested. In line with these findings, a previous study designed to identify genomic predictors of response to taxane–anthracycline chemotherapy identified *NFIB* as a predictor gene for residual disease in ER-negative breast cancer [45]. The effect of NFIB depletion on docetaxel response was accompanied by p21 induction, with p21 being critical to docetaxel-induced growth inhibition. Thus, our results indicate that NFIB depletion sensitises TNBC cancer cells to chemotherapeutic agents such as docetaxel in a p53-independent, but p21-dependent, manner. Notably, we found that low levels of *NFIB*, but not high levels of *NFIB*, were associated with increased survival in patients treated with chemotherapy compared with patients who did not receive chemotherapy. It will be important to pursue this finding using a larger cohort of patients to specifically address the predictive power of NFIB in breast cancer chemotherapy.

While there is accumulating evidence supporting apoptotic and chemotherapy-sensitising roles for p21 that are independent of p53 [40,46], the mechanism underlying p21-mediated docetaxel cytotoxicity in our TNBC cells remains unclear. In light of our observation that cleaved caspase 3 is induced upon NFIB depletion in TNBC, we suggest that p21 enhances apoptosis in TNBC cells treated with docetaxel by directly or indirectly inducing pro-apoptotic factors such as cleaved caspase 3. In keeping with this idea, ectopic expression of p21, along with enhanced chemosensitivity and increased apoptosis (as measured by cleaved caspase 3), has been reported in other cancer cell lines [46].

In summary, our study suggests that NFIB drives cell survival and drug resistance in TNBC, leading to aggressive growth, tumour progression, and poor clinical outcomes. As NFIB depletion restores p21 function in *TP53*-mutated TNBC cells, targeting NFIB represents a potential therapeutic intervention for TNBC patients.

Acknowledgements

We thank Kathryn Graham and Adrian Driga for their help with gene profiling database management; Darryl Glubrecht for his help with the immunostaining of breast cancer tissue sections; and Dr Naomi Tanese, New York University School of Medicine, for her kind donation of the anti-NFI antibody used for our gel shift assays. The mouse monoclonal 3B5 AP-2 α (TFAP2A) antibody, developed by TJ Williams, University of Colorado, was obtained from the Developmental Studies Hybridoma Bank, created by the NICHD of the NIH and maintained

at The University of Iowa, Department of Biology, Iowa City, IA, USA. This work was supported by grants from the Canadian Institutes of Health Research (grant No 130134) and the Canadian Cancer Society Research Institute (grant No 705455).

Author contributions statement

RZL conceived and carried out experiments, analysed the data, and drafted the manuscript. TMV, SJ, WSC, EG, and EAM carried out experiments. JRM was involved in the study design and data collection. RG was involved in the study design, data interpretation, and manuscript editing. All authors reviewed and approved the manuscript.

References

- Onitilo AA, Engel JM, Greenlee RT, et al. Breast cancer subtypes based on ER/PR and Her2 expression: comparison of clinicopathologic features and survival. *Clin Med Res* 2009; **7**: 4–13.
- Yeo B, Turner NC, Jones A. An update on the medical management of breast cancer. *BMJ* 2014; **348**: g3608.
- Shah SP, Roth A, Goya R, et al. The clonal and mutational evolution spectrum of primary triple-negative breast cancers. *Nature* 2012; **486**: 395–399.
- Turner N, Moretti E, Siclari O, et al. Targeting triple negative breast cancer: is p53 the answer? *Cancer Treat Rev* 2013; **39**: 541–550.
- Walerych D, Napoli M, Collavin L, et al. The rebel angel: mutant p53 as the driving oncogene in breast cancer. *Carcinogenesis* 2012; **33**: 2007–2017.
- Fane M, Harris L, Smith AG, et al. Nuclear factor one transcription factors as epigenetic regulators in cancer. *Int J Cancer* 2017; **140**: 2634–2641.
- Gronostajski RM. Roles of the NFI/CTF gene family in transcription and development. *Gene* 2000; **249**: 31–45.
- Murtagh J, Martin F, Gronostajski RM. The nuclear factor I (NFI) gene family in mammary gland development and function. *J Mammary Gland Biol Neoplasia* 2003; **8**: 241–254.
- Becker-Santos DD, Lonergan KM, Gronostajski RM, et al. Nuclear factor I/B: a master regulator of cell differentiation with paradoxical roles in cancer. *EBioMedicine* 2017; **22**: 2–9.
- Chen KS, Lim JWC, Richards LJ, et al. The convergent roles of the nuclear factor I transcription factors in development and cancer. *Cancer Lett* 2017; **410**: 124–138.
- Piper M, Barry G, Harvey TJ, et al. NFIB-mediated repression of the epigenetic factor Ezh2 regulates cortical development. *J Neurosci* 2014; **34**: 2921–2930.
- Steele-Perkins G, Plachez C, Butz KG, et al. The transcription factor gene *Nfib* is essential for both lung maturation and brain development. *Mol Cell Biol* 2005; **25**: 685–698.
- Denny SK, Yang D, Chuang CH, et al. Nfib promotes metastasis through a widespread increase in chromatin accessibility. *Cell* 2016; **166**: 328–342.
- Dooley AL, Winslow MM, Chiang DY, et al. Nuclear factor I/B is an oncogene in small cell lung cancer. *Genes Dev* 2011; **25**: 1470–1475.
- Semenova EA, Kwon MC, Monkhurst K, et al. Transcription factor NFIB is a driver of small cell lung cancer progression in mice and marks metastatic disease in patients. *Cell Rep* 2016; **16**: 631–643.
- Wu N, Jia D, Ibrahim AH, et al. NFIB overexpression cooperates with *Rb/p53* deletion to promote small cell lung cancer. *Oncotarget* 2016; **7**: 57514–57524.
- Han W, Jung EM, Cho J, et al. DNA copy number alterations and expression of relevant genes in triple-negative breast cancer. *Genes Chromosomes Cancer* 2008; **47**: 490–499.
- Moon HG, Hwang KT, Kim JA, et al. NFIB is a potential target for estrogen receptor-negative breast cancers. *Mol Oncol* 2011; **5**: 538–544.
- Smith DD, Saetrom P, Snove O Jr, et al. Meta-analysis of breast cancer microarray studies in conjunction with conserved *cis*-elements suggests patterns for coordinate regulation. *BMC Bioinformatics* 2008; **9**: 63.
- Liu RZ, Graham K, Glubrecht DD, et al. Association of FABP5 expression with poor survival in triple-negative breast cancer: implication for retinoic acid therapy. *Am J Pathol* 2011; **178**: 997–1008.
- The Cancer Genome Atlas Network. Comprehensive molecular portraits of human breast tumours. *Nature* 2012; **490**: 61–70.
- Pereira B, Chin SF, Rueda OM, et al. The somatic mutation profiles of 2,433 breast cancers refines their genomic and transcriptomic landscapes. *Nat Commun* 2016; **7**: 11479.
- Liu RZ, Garcia E, Glubrecht DD, et al. CRABP1 is associated with a poor prognosis in breast cancer: adding to the complexity of breast cancer cell response to retinoic acid. *Mol Cancer* 2015; **14**: 129.
- Mita R, Coles JE, Glubrecht DD, et al. B-FABP-expressing radial glial cells: the malignant glioma cell of origin? *Neoplasia* 2007; **9**: 734–744.
- Ouellet S, Vigneault F, Lessard M, et al. Transcriptional regulation of the cyclin-dependent kinase inhibitor 1A (p21) gene by NFI in proliferating human cells. *Nucleic Acids Res* 2006; **34**: 6472–6487.
- Liu RZ, Graham K, Glubrecht DD, et al. A fatty acid-binding protein 7/RXR β pathway enhances survival and proliferation in triple-negative breast cancer. *J Pathol* 2012; **228**: 310–321.
- Bisgrove DA, Monckton EA, Packer M, et al. Regulation of brain fatty acid-binding protein expression by differential phosphorylation of nuclear factor I in malignant glioma cell lines. *J Biol Chem* 2000; **275**: 30668–30676.
- Brun M, Glubrecht DD, Baksh S, et al. Calcineurin regulates nuclear factor I dephosphorylation and activity in malignant glioma cell lines. *J Biol Chem* 2013; **288**: 24104–24115.
- Germain DR, Graham K, Glubrecht DD, et al. DEAD box 1: a novel and independent prognostic marker for early recurrence in breast cancer. *Breast Cancer Res Treat* 2011; **127**: 53–63.
- Bullwinkel J, Baron-Luhr B, Ludemann A, et al. Ki-67 protein is associated with ribosomal RNA transcription in quiescent and proliferating cells. *J Cell Physiol* 2006; **206**: 624–635.
- Bianco S, Jangal M, Garneau D, et al. LRH-1 controls proliferation in breast tumor cells by regulating *CDKN1A* gene expression. *Oncogene* 2015; **34**: 4509–4518.
- De Santi M, Galluzzi L, Lucarini S, et al. The indole-3-carbinol cyclic tetrameric derivative CTet inhibits cell proliferation via overexpression of p21/CDKN1A in both estrogen receptor-positive and triple-negative breast cancer cell lines. *Breast Cancer Res* 2011; **13**: R33.
- Jagadish N, Gupta N, Agarwal S, et al. Sperm-associated antigen 9 (SPAG9) promotes the survival and tumor growth of triple-negative breast cancer cells. *Tumour Biol* 2016; **37**: 13101–13110.
- Chavez KJ, Garimella SV, Lipkowitz S. Triple negative breast cancer cell lines: one tool in the search for better treatment of triple negative breast cancer. *Breast Dis* 2010; **32**: 35–48.
- Fernandes-Alnemri T, Litwack G, Alnemri ES. CPP32, a novel human apoptotic protein with homology to *Caenorhabditis elegans* cell death protein Ced-3 and mammalian interleukin-1 beta-converting enzyme. *J Biol Chem* 1994; **269**: 30761–30764.
- Kashiwagi E, Izumi H, Yasuniwa Y, et al. Enhanced expression of nuclear factor I/B in oxaliplatin-resistant human cancer cell lines. *Cancer Sci* 2011; **102**: 382–386.

37. Brun M, Coles JE, Monckton EA, *et al.* Nuclear factor I regulates brain fatty acid-binding protein and glial fibrillary acidic protein gene expression in malignant glioma cell lines. *J Mol Biol* 2009; **391**: 282–300.
38. Harris L, Genovesi LA, Gronostajski RM, *et al.* Nuclear factor one transcription factors: divergent functions in developmental versus adult stem cell populations. *Dev Dyn* 2015; **244**: 227–238.
39. Ghabach B, Anderson WF, Curtis RE, *et al.* Adenoid cystic carcinoma of the breast in the United States (1977 to 2006): a population-based cohort study. *Breast Cancer Res* 2010; **12**: R54.
40. Abbas T, Dutta A. p21 in cancer: intricate networks and multiple activities. *Nat Rev Cancer* 2009; **9**: 400–414.
41. Shoji T, Tanaka F, Takata T, *et al.* Clinical significance of p21 expression in non-small-cell lung cancer. *J Clin Oncol* 2002; **20**: 3865–3871.
42. Rose SL, Goodheart MJ, Deyoung BR, *et al.* p21 expression predicts outcome in p53-null ovarian carcinoma. *Clin Cancer Res* 2003; **9**: 1028–1032.
43. Isakoff SJ. Triple-negative breast cancer: role of specific chemotherapy agents. *Cancer J* 2010; **16**: 53–61.
44. Alken S, Kelly CM. Benefit risk assessment and update on the use of docetaxel in the management of breast cancer. *Cancer Manag Res* 2013; **5**: 357–365.
45. Hatzis C, Pusztai L, Valero V, *et al.* A genomic predictor of response and survival following taxane–anthracycline chemotherapy for invasive breast cancer. *JAMA* 2011; **305**: 1873–1881.
46. Liu S, Bishop WR, Liu M. Differential effects of cell cycle regulatory protein p21^{WAF1/Cip1} on apoptosis and sensitivity to cancer chemotherapy. *Drug Resist Updat* 2003; **6**: 183–195.

SUPPLEMENTARY MATERIAL ONLINE

Figure S1. *NFIB* expression correlates with tumour histological grade and patient prognosis

Figure S2. *NFI* RNA levels in a panel of breast cancer cell lines

Figure S3. Effect of *NFIB* overexpression on cellular response to docetaxel

Figure S4. A schematic illustration of the role of *NFIB* in breast cancer

Table S1. Nucleotide sequences of PCR primers and siRNAs

Table S2. Clinicopathological associations of *NFI* mRNA levels in human breast cancer